IEEE Journal of Translational Engineering in Health and Medicine

Received 17 December 2017; revised 1 April 2018; accepted 2 May 2018.
Date of publication 21 May 2018; date of current version 5 June 2018.

Digital Object Identifier 10.1109/JTEHM.2018.2837895

A Locomotion Control Platform With Dynamic Electromagnetic Field for Active Capsule Endoscopy

FAHAD N. ALSUNAYDIH, (Student Member, IEEE), JEAN-MICHEL REDOUTÉ, (Senior Member, IEEE), AND MEHMET R. YUCE, (Senior Member, IEEE)

Department of Electrical and Computer Systems Engineering, Monash University, Melbourne, VIC 3800, Australia

CORRESPONDING AUTHOR: F. N. ALSUNAYDIH (fahad.alsunaydih@monash.edu)

The work of F. N. Alsunaydih was supported by the Saudi Arabian Cultural Mission, Australia. The work of M. R. Yuce was supported by the Australian Research Council Future Fellowships under Grant FT130100430.

ABSTRACT Conventional radiological and endoscopic techniques utilizing long tubes were ineffective in visualizing the small bowel mucosa until the development of wireless capsule endoscopy (WCE). WCE is a revolutionary endoscopic technology that can diagnose the complete gastrointestinal tract. However, the existing capsule technologies are passive, and thus they cannot be navigated to or held in a specific location. The design of an active capsule will present the opportunity to move and stop a device at any targeted locations leading to numerous medical applications such as drug delivery or collecting tissue samples for examinations in the laboratory. This paper implements a new locomotion methodology for WCE systems using an electromagnetic platform. The platform produces a dynamic electromagnetic field to control the motion of the capsule. The strength and the direction of the electromagnetic field that is generated by the platform are continuously adjusted in order to maintain the equilibrium state during the capsule movement. We present the detailed design of the proposed platform with an experimental setup with polyvinyl chloride tubes and *ex vivo* to demonstrate the performance of the capsule motion.

INDEX TERMS Wireless capsule endoscopy, electromagnetic platform, equilibrium state, capsule locomotion.

I. INTRODUCTION

The development of Wireless Capsule Endoscopy (WCE) systems started in 2000, primarily targeting the diagnosis and management of various small intestine diseases [1]. The capsule that the patient swallows is the size of a multivitamin pill; when used for diagnosis of the GI tract, it causes no pain and can reach the small intestine, whereas an ordinary endoscopy is limited to the stomach and to the colon. Wireless capsules commercially available are passive, which means that they move only by peristalsis and the contractions of organs. In addition to capturing images, a wireless capsule controlled in the body could have a wide range of medical applications such as drug delivery or sample collection from part of the GI tract for testing. Leung *et al.* [2] proposed an inflatable capsule that has a balloon structure to stop the bleeding in the small intestine. For an active WCE, the velocity of a capsule moving within the body is important to allow clear and sufficient pictures. With existing capsule devices, a single patient produces nearly 50,000 images per examination, and physicians require an average of 2 hours to evaluate the video recordings. Thus, costs incurred through WCE use are higher than those of traditional endoscopic methods. A system that can effectively provide an accurate motion with steady steps chosen by the physician is therefore desirable to control the landing of the capsule inside the GI tract. In practice, such a system will allow the capsule to pause at any specific location and move at a high and changeable velocity convenient to the GI tract movements, as described in [3].

Several techniques have been developed to control the motility of a capsule within the human digestive system [4]. An earthworm-like mechanism that uses shape memory alloy (SMA) operation based on a stretching, contracting, and

holding mechanism was proposed to achieve a motion with 9.6 mm/min velocity [5]. Another legged-based method uses a DC motor inside the capsule to actuate the legs at a velocity of 50 mm/min [6]. The main disadvantages of the internal locomotion mechanisms are their high power-consumption requirements and their low ranges of velocity. Other methods are based on externally controlled mechanisms that use an external magnetic field to manipulate a capsule within the body. These methods have been investigated using a permanent magnet within the capsule body. The method presented in [8] uses a robotic arm with a permanent magnet at the end of the arm. The robotic arm's mechanical movement is reflected to the permanent magnet inside the capsule, and thus the capsule will follow the robotic arm. Similarly, a hand-held external controller method using an external permanent magnetic was proposed in [9] to manipulate the capsule. The most promising methods have been those based on electromagnetic actuation, which provides a sufficient force for control of capsule motion by varying the excitation current. The electromagnetic field produced by electromagnets is safe for the human body because the intensity and the frequency are sufficiently low. A spiral-like capsule design controlled by rotational electromagnetic fields was fabricated to move a capsule within the GI tract [7]. The design is not able to maintain a specific position and presents a high risk of twisting in the small intestine. Keller *et al.* [11] proposed a six pairs of coils to control the capsule in a water-filled stomach only. ALICE system which uses five pairs of coils to perform a helical motion by combining the translation and the rotational motion was proposed in [12].

As a capsule's limited size makes power consumption a critical factor, the proposed method in this research requires no additional power within the capsule to enable the motion. The proposed system in this paper does not rely on human skill, as it can be operated automatically using appropriate feedback to navigate the capsule [13], [15]. The mechanism takes advantage of the electromagnetic field superposition concept, with the total electromagnetic field and the total magnetic force to establish motion control. Unlike systems in previous studies that use the electromagnetic platform, the motion of the proposed system is based on what we call "digital movement" rather than the need of a mechanical involvement in the platform or performing helical motion in the existing designs available in the literature. Also, this system can effectively be used in both stomach and small intestine. As Section II will describe, the digital movement is governed by a current square pulse that results in precise steps along the desired direction. Specifically, the step's size and the frequency of the steps are also controllable, giving the physician the ability to choose the velocity and precisely landing the capsule at any distance in a new position.

II. IMPLEMENTATION OF LOCOMOTION METHOD WITH DYNAMIC ELECTROMAGNET FIELD

The locomotion system proposed in this research comprises two stationary sets of parallel and identical electromagnets

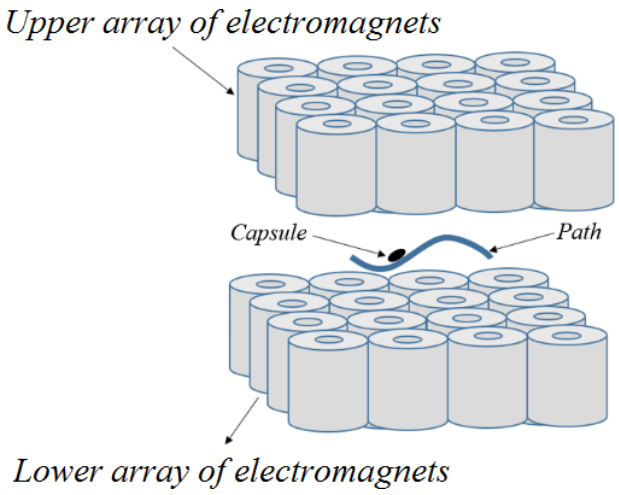

FIGURE 1. The proposed WCE locomotion system.

that are placed underneath and above the targeted area, as Fig.1 shows. This configuration has a total working area of $15 \times 15cm^2$ and can be enlarged by increasing the number of electromagnets. We chose this arrangement to reduce the attractive force perpendicular to the path, which could damage the tissue as described in [16]. Shaping the electromagnetic field components to stretch the total length of the field along the direction of the motion is key to the design. The proposed arrangement produces electromagnetic forces compounded of the actuation forces from each source and that are sufficient to overcome resistive forces such as friction and the partial obstructions in the small bowel, which Section II will describe. Moreover, the configuration provides a higher level of safety because no mechanical movement is required to manipulate a capsule. We have implemented a prototype to validate the theoretical approach with practical measurements. To make the capsule follow the electromagnetic field produced by the electromagnets, we embedded a 2.8-mm-height and 8-mm-diameter (N52) permanent magnet in the capsule.

We evaluated the locomotion strategy of the capsule in this paper to demonstrate a new method to obtain controllable motion and velocity by switching the electromagnets for a different period and by changing the rate of the switching per unit time. One advantage of a changeable motion speed is that the consistency improves between the GI tract and the capsule movement. It also allows the physician to choose the required number of images per unit distance/time.

A. MODELING OF ELECTROMAGNETIC FIELDS AND FORCES

To achieve this method's primary goal, the kinematic properties of the workspace should be analyzed to describe the capsule's motion. Initially, consider that the capsule is placed at the center and above an electromagnet $(0, y, 0)$. The coordinates of the force can be written as

$$\vec{r} = (0i + yj + 0k) \tag{1}$$

IEEE Journal of Translational Engineering in Health and Medicine

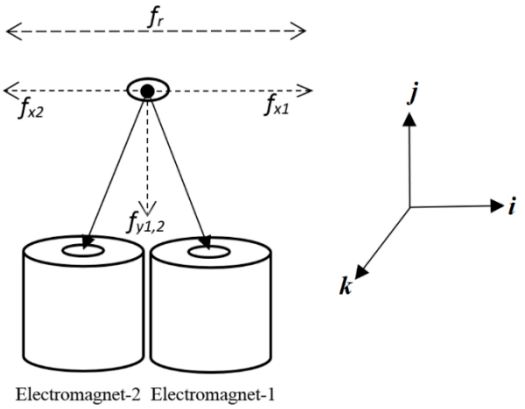

FIGURE 2. Forces exerted by two adjacent electromagnets on the capsule.

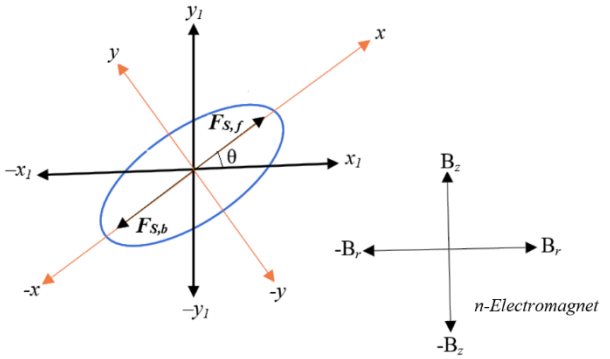

FIGURE 3. Free body diagram of the capsule.

where y represents the vertical placement. Then, if the capsule is horizontally placed above and between two electromagnets, as Fig. 2 shows, the coordinates of the forces at any horizontal displacement become

$$\vec{r} = (\mathrm{x}i + yj + 0k) \tag{2}$$

where x represents the horizontal placement. Hence, the required force for the motion at any horizontal direction (i.e. toward electromagnet-1) can be expressed as

$$F_s = F_{x1} - F_{x2} - F_r \tag{3}$$

where F_s is the motion force, Fx_1 is the radial force exerted by electromagnet-1, Fx_2 is the radial force exerted by electromagnet-2, and F_r is the friction force.

Fundamentally, two main factors affect the nomination of the motion force to obtain the required motion precision and velocity: the duration of the current pulse used to switch off the electromagnet and the rate of the current pulses per unit time. The first factor controls the motion precision, whereas both factors affect the velocity of the motion. To control the motion of the capsule in a differentiable path, we assume that the arbitrary location of the capsule is $P = (x + y + z)$. The unit tangent vector that represents the direction of the motion can be found by differentiating the individual coordinates as:

$$\vec{T} = \frac{P'}{\|P'\|} \tag{4}$$

where $\vec{T}$ is the unit tangent vector and P is the location of the capsule. This expression is known as the Frenet–Serret formula and is valid for infinitesimal as the curve can be expressed as a straight line. This expression becomes important when the applied current to each electromagnet must be regulated to produce the required electromagnetic field according the location and the direction of the capsule's motion. Fig.9 shows the expression's uses. Fig.3 shows the free body diagram of the capsule.

The (x, y) plane represents the direction of the motion, whereas the $(x1, y1)$ plane represents the radial and axial components of the electromagnetic field (Br, Bz) with respect to the electromagnetic plane. The total electromagnetic force applied to the capsule can be determined using the superposition principle because the total electromagnetic force component is the sum of each electromagnetic force, as illustrated in (5):

$$\boldsymbol{F}_{s(f,b)} = V\left(\nabla \cdot \left(M_{r,z}\sum_{i=1}^{n} \pm B_{r,n}\cos\theta + M_{r,z}\sum_{i=1}^{n} \pm B_{z,n} sin\,\theta\right)\right) \tag{5}$$

where $F_{s(f,b)}$ is the motion force in the forward and backward direction, V is the volume of the permanent magnet, $M_{r,z}$ are the magnetization components of the permanent magnet embedded into the capsule that are assumed to be constant, $B_{z,n}$ and $B_{r,n}$ are the axial and radial electromagnetic fields of individual electromagnets applied to the capsule, and θ is the angle between the capsule plane and the electromagnets plane, as shown in Fig. 3.

The electromagnetic field components B_z and B_r can be found using the following equations:

$$B_r = -\frac{a\mu ni}{2\pi}\int_0^{\pi}\left[\frac{\cos\,\emptyset d\emptyset}{\sqrt{\xi^2 + r^2 + a^2 - 2ar\,\cos\emptyset}}\right]_{\xi_-}^{\xi_+} \tag{6}$$

$$B_z = \frac{a\mu ni}{2\pi}\int_0^{\pi} \times\left[\frac{\xi(a - r\,\cos\emptyset)d\emptyset}{(r^2 + a^2 - 2ar\,\cos\emptyset)\sqrt{\xi^2 + r^2 + a^2 - 2ar\,\cos\emptyset}}\right]_{\xi_-}^{\xi_+} \tag{7}$$

where a is the radius of the electromagnet, n is the number of turns per unit length, i is the current flowing in the electromagnet, μ is permeability, r is the radial distance, $\xi = z \pm L/2$ where z is the axial distance for the electromagnet, and L is the length of the electromagnet. Based on the above equations, the total electromagnetic field of each electromagnet is $B_T = \sqrt{B_z^2 + B_r^2}$, and the direction angle θ is $= \tan^{-1}(B_z/B_r)$. The electromagnetic field can be calculated precisely at any chosen point $P(r, z)$ using the finite element method (FEM) or equations (6) and (7) to understand the distribution and thus generate the electromagnetic field according to the shape of the path.

It is convenient to use equations (6) and (7) because of the flexibility of changing the parameters of the system and in case of real-time calculations where the processing time need to be as instant as possible. One way to reduce the computation effort is to express the electromagnetic field produced by each electromagnet by the mean of the current flowing into it because the relationship between them is linear. However, in the present system, iron is used as the core material to enhance the electromagnetic field intensity, but the permeability of iron is not linear.

Various practical and mathematical methods can approximate the magnetization, but the results obtained are either inaccurate or overly complex. In our analytical approach, we used the numerical data the core manufacturer provided as a lookup table with the help of piecewise linear approximation to find the magnetization of the iron core at any given current. As a result, this work uses MATLAB to calculate the contribution of each electromagnet in the platform and sum it up linearly according the position and the direction of the motion, as shown in Equation 5.

If the capsule moves in a horizontal path and between two electromagnets, as Fig. 4 shows, the forces that have impact on the capsule motion are the summation of the radial components from each electromagnet $\sum_{i=1}^{n} B_{r,n}$ because the magnitude of the tangent vector is 1 with respect to the electromagnet's plane. The forces applied to the capsule in both directions must be equal to keep the capsule in equilibrium. On the other hand, the total axial components from each electromagnet $\sum_{i=1}^{n} B_{z,n}$ contribute to the total force of the motion if the capsule moves along a differential path. In such a case, the total motion force $F_{s(f,b)}$ must be sufficient to overcome new parameters such as weight. Hence, we can determine the static equilibrium state by balancing between the friction force, electromagnetic force, and weight as follows:

$$F_{s(f,b)} - \mu_f \cos\theta - mg \sin\theta = 0 \tag{8}$$

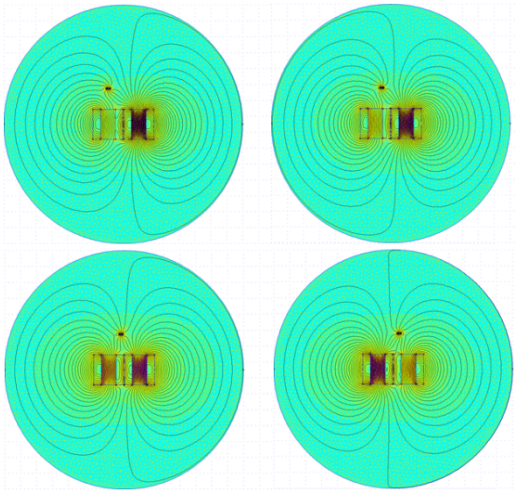

FIGURE 4. Effect of each electromagnetic field at the permanent magnet inside the capsule using FEM Simulation.

where m is the mass of the capsule, g is the gravity acceleration, μ_f is the friction coefficient, and θ is the inclination angle measured from the x-axis of the path to the x-axis of the platform.

B. MOTION CONTROL STRATEGY

The setup described in the previous section uses a controller to perform the control strategy of this mechanism. The algorithm used in this paper performs two operations. The first form is the static form, where the system controls the electromagnet's currents to produce a constant electromagnetic field to reach the equilibrium to hold the capsule according to its position within the workspace. The second form is the dynamic form, where the system applies a current pulse to the electromagnets to start the motion at the chosen direction, step size, and velocity.

As Fig.5 shows, the first step of the proposed algorithm is to reach and maintain the equilibrium state in the absence of the current pulse by applying a static electromagnetic field from the stationary electromagnets according to the location of the capsule within the workspace. To start the motion, the system switches to the dynamic form by using the pre-calculated current pulses and applying them to the electromagnet that is opposite to the direction of the motion. The current pulse basically will change the status of the applied current from high to low. Hence, the direction of the total net force will be changed from the equilibrium state to the direction of the motion. The current pulse concept significantly improves the accuracy and the control over the velocity. For example, as Fig. 6 shows if the motion is directed toward electromagnet-2, current pulses will be applied to electromagnet-1 to eliminate the force from its direction, which causes the capsule to follow the force from electromagnet-2. The system in this paper is dynamic and it has no thresholds as the environment of the workspace (i.e., small intestine) is not predictable (different geometries

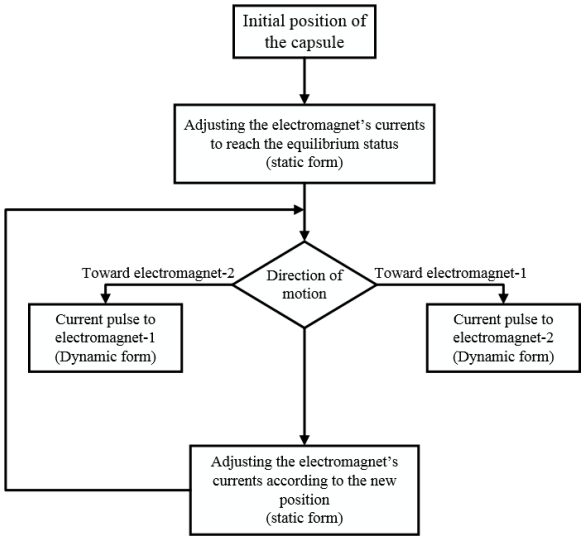

FIGURE 5. Flow chart shown the algorithm of the motion mechanism.

IEEE Journal of Translational Engineering in Health and Medicine

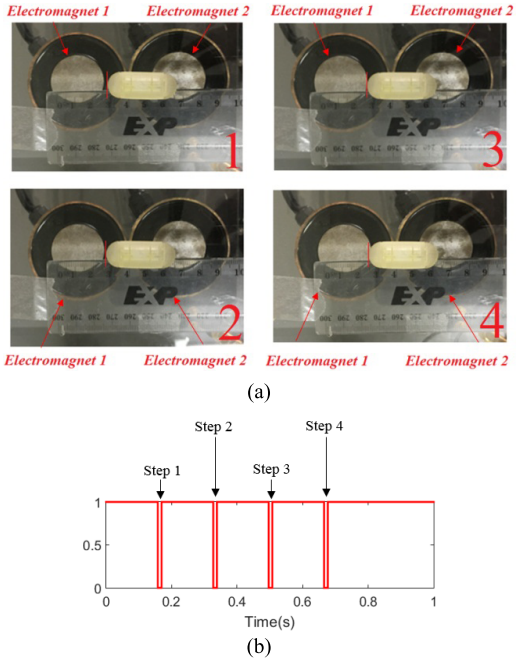

FIGURE 6. **(a) The motion of the capsule at 1mm step size (four steps). (b) The current pulses associated with each step.**

and resistive forces). Hence, we intended to generalize the method in a way that can manage any environment by switching between the static and dynamic modes.

As the duration of the current pulse defines the step size of the motion and can be modified according the physician's requirements, the parameters that must be considered are the mass of the capsule, the required step size, and the applied force, as shown in (9):

$$t = \sqrt{\frac{d.m.2}{F_{s(f,b)}}} \tag{9}$$

where t is the duration of the low state of the current pulse, d is the step size, m is the mass of the capsule. With this method, one step has been created that can be chosen in terms of velocity and resolution. After that, the control system will switch to the static form. In this form, new values of currents will be applied to the electromagnets to modify the total electromagnetic field to reach the equilibrium state at the new position. This process provides the flexibility to change or maintain the step size for each step. The results section will explain the second factor that influences the velocity.

C. HARDWARE AND CALIBRATION

The system contains eight electromagnets: four electromagnets for each platform, depicted schematically in Fig. 7. The electromagnet's diameter is 75mm, and the length is 75mm. The power supply used in this setup is Aim-ttiQPX600D (80V, 60A) which has two independent outputs, each of which can deliver up to 6kW.

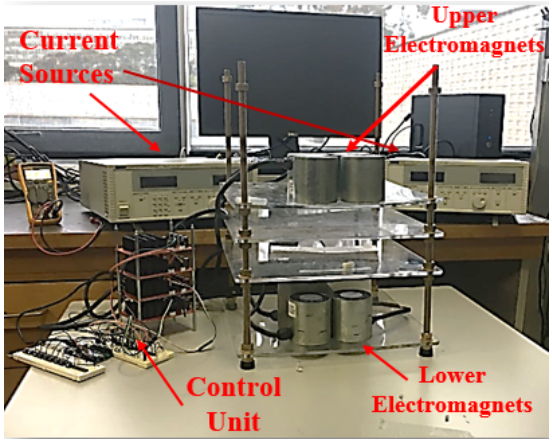

FIGURE 7. **The mechanism setup.**

We arranged a power MOSFET transistor as an H-bridge to control the switching and the amount of current of each electromagnet, which is accomplished by delivering variable PWM periods. The purpose of using this setup was to apply the simulated current values obtained with MATLAB using equations (6) and (7) to control the motion of the capsule digitally and automatically. A calibration process also was required for each electromagnet because of manufacturing imperfections and the materials surrounding the setup. Calibration involved applying a known amount of current to produce the expected electromagnetic field. The error in the electromagnetic field values was then used as a correction factor for scaling the electromagnetic fields and matching them to the data obtained theoretically using a SS49E linear Hall-effect sensor. The results showed that the mean error values of each electromagnet were between 0.2-0.7 mT with no standard deviation higher than mean error which means that data is not highly skewed. This hypothesis was important to assure that the applied electromagnetic fields were highly accurate to perform the motion precisely.

III. EXPERIMENTAL RESULTS

We performed several tests using PVC tubes with 25mm diameter with different shapes and lengths to verify the proposed mechanism. We first implemented capsule motion on the horizontal path between two electromagnets as a primary element, as shown in Fig. 6. We then performed a configuration that varied the inclination angle, as Fig. 10 shows, to test the motion on differential paths. Finally, we tested the system *ex-vivo* to validate the mechanism in a real environment scenario. Further, we performed different tests to verify the motion precision and also to verify that the total field generated from the array of electromagnets could overcome the resistive forces that could present in the path. The total electromagnetic field is not fixed, it depends on the position of the capsule, the orientation, the resistive forces and the speed. During the implementation, we found that the size of the electromagnets did not affect the motion precision but

that their electromagnetic field intensity was lower. In our setup, we choose the workspace height to be 160mm as shown in Fig.10. Hence, and based on the simulations and experiments, we found that the 75mm electromagnet can produce the required field intensity for mobility without producing much heat from the electromagnets. The amount of the electromagnetic field produced by each electromagnet depends on the position of the capsule with respect to each electromagnet and the geometry of the electromagnet.

Fig.8 shows the basic concept of controlling the motion in different directions using an array of electromagnets in each platform. In case of horizontal motion (i.e., $\theta = 0$), the electromagnets in the lower platform produce most of the force necessary to move the capsule, whereas the electromagnets in the upper platform have a lower impact and are used to reduce the force perpendicular to the path, which could damage the GI tract, and, if required, boost the force parallel to the path. As the inclination angle increases (i.e., $\theta > 0$), the electromagnets in the upper platform play a major role in moving the capsule by reshaping the electromagnetic field to align with the path while maintaining zero net force.

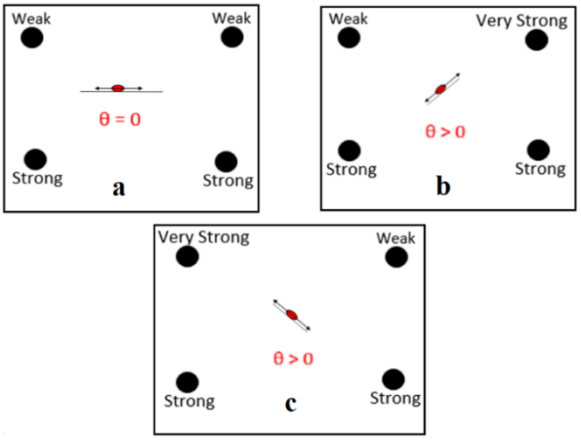

FIGURE 8. Controlling the motion in different directions. The upper dots represent the upper platform of the system whereas the lower dots represent the lower platform.

This system implemented no feedback from the location or path's orientation, but the total distance by means of the known number and the size of steps can accurately verify the mechanism. The control system treads the motion along the path point by point such that the electromagnetic field from each electromagnet is regulated according to the capsule's location and orientation. Fig. 9 shows the total electromagnetic field applied to move the capsule along the horizontal path and between two electromagnets as shown in Fig. 6. When the capsule is in the middle point between the two electromagnets (i.e., 37.5mm), the electromagnetic fields are equal in magnitude and opposite in direction to maintain the equilibrium.

For a differential path, as the angle of inclination starts changing, the electromagnetic fields from the upper platform will contribute first to overcoming the effect of the gravity ($mg\ sin\theta$), and second to aligning the capsule with the path axis, as described in Section II. In that regard, we performed several tests to verify the proposed mechanism and evaluate the motion precision. We modified the PVC tube used in this system with heat to represent a differential path, as Fig.10 shows.

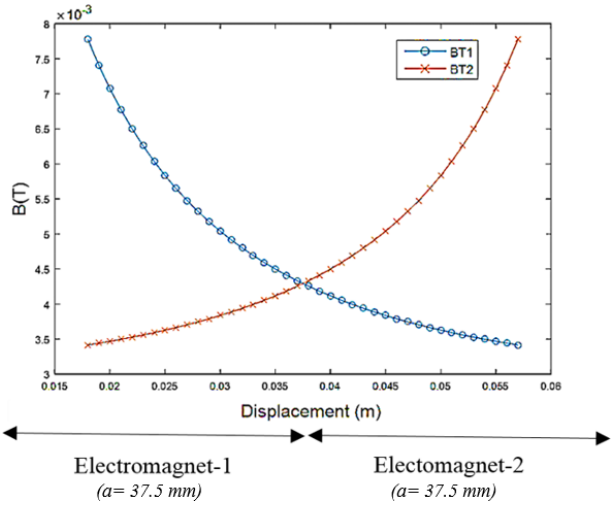

FIGURE 9. The electromagnetic field applied from electromagnet-1 and electromagnet-2 to move the capsule in horizontal path (i.e. $\theta = 0$) as shown in the configuration in Fig.7.

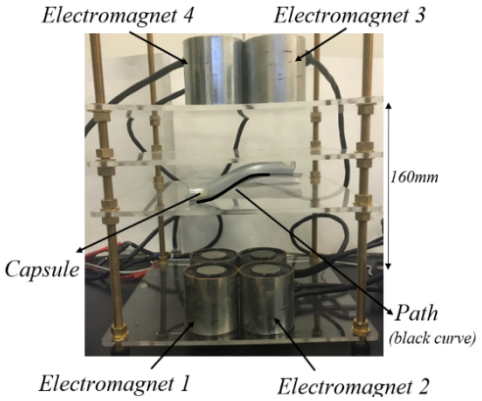

FIGURE 10. The actual setup used to conduct the method with differential path.

We then simulated the path geometry in MATLAB to calculate the required electromagnetic field for any given location and from which direction it must be applied. The combination of the selected step size and the direction of the tangent vector give the exact location along the differential curve as Fig.11 shows.

For the case shown in Fig. 10, the amount of contribution from electromagnet-3 increases as angle θ increases to reach the equilibrium status by aligning the total electromagnetic field with the vector that is tangent to the path. Hence, the total electromagnetic field in the forward direction $B_{sf} = \sum B_{r2,3}\, cos\theta + B_{z3}\, sin\theta$ must be equal to the total electromagnetic field in the reverse direction

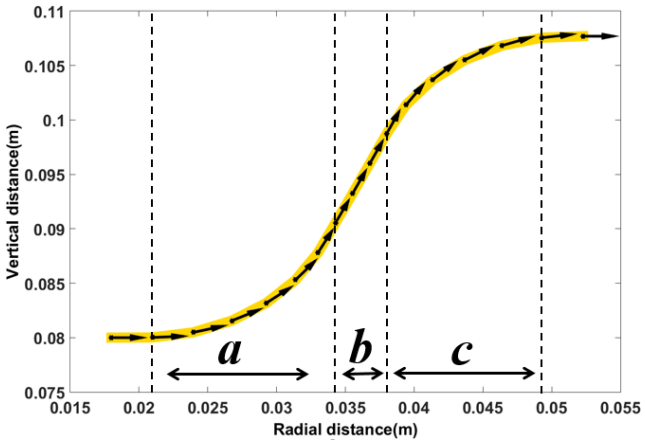

FIGURE 11. The simulation of the path in MATLAB. The black arrows inside the path are from the application of Frenet–Serret formula.

$B_{sb} = \sum B_{z1,2}\, sin\theta + B_{r1}\, cos\theta$. In other words, the contribution of the axial component of the electromagnetic field in electromagnet-1, electromagnet-2 and electromagnet-3 becomes larger as the inclination angle increases, while the radial component governs the motion as θ become smaller, as Fig. 12 shows.

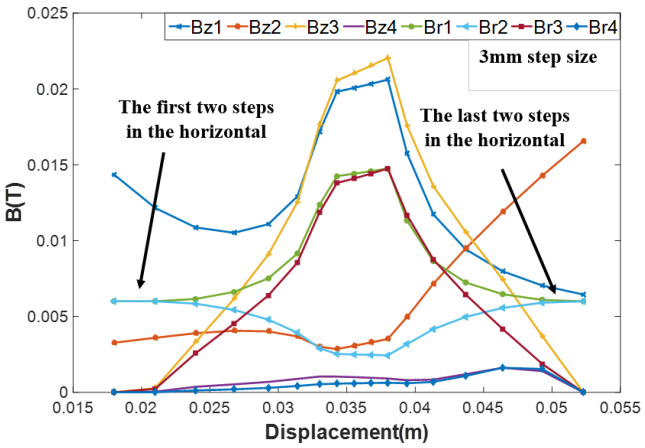

FIGURE 12. *Br* and *Bz* components of the electromagnets at each step for the case shown in Fig.11.

Fig. 12 also shows that the radial components of the electromagnetic field B_{r1} and B_{r2} are always equal when the capsule is in the horizontal path, as in the first two steps and the last three steps in this case. On the other hand, the axial component of electromagnet-3 increases gradually to balance the capsule in the inclined path and overcomes the weight as a new parameter. Importantly, the total force in both directions must include the friction force and the weight according to the path geometry.

We measured the total field applied in the capsule in both forward/backward directions with respect to its plane using a SS49E linear Hall-effect sensor, as Fig. 13 shows. Also, we calculated the simulated total field in the same figure by subtracting the total electromagnetic field components from each source in forward direction B_{sf} from the total electromagnetic field in the reverse direction B_{sb}. Fig.13 also shows the correlation in equilibrium status of the endoscopic capsule along the path in simulation and measurement.

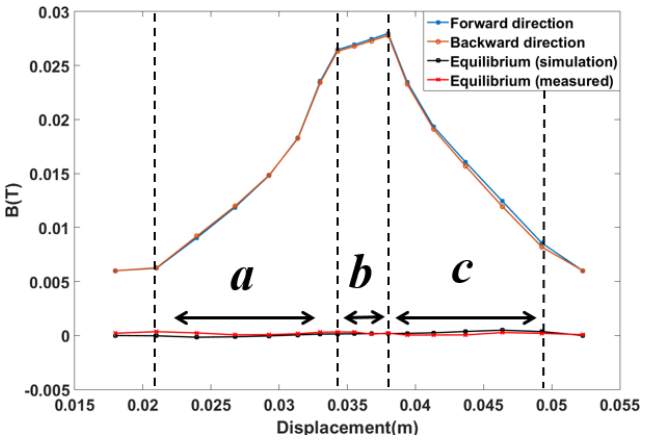

FIGURE 13. The total electromagnetic field in the forward direction B_{sf} and in the reverse direction B_{sb} and the comparison between simulations and measurements. It also shows the impact of the angle of inclination during its motion in phase a, b and c.

In the control system used in this case, and according to (8), one can see the increment of the total force in relation to the angle of inclination by comparing Fig.11 and Fig.13. In the first few steps, where the path is horizontal, the total force has been kept low, but it is sufficient to move the capsule. In phase (a), where θ gradually increases with each step, the total force also increases gradually. After that, we reduced the incrementing of the angle of inclination for a few steps and verify the total force, as appears in phase (b). Phase (c) shows the total force when the angle of inclination begins decrementing steadily.

During the measurements, we noticed a small variation in the total electromagnetic field between the simulation and result even after calibration; however, this variation ranged from -0.21 mT to 0.33 mT, which is negligible compared with the total electromagnetic field. This could occur because of the position of the sensor during the measurements as the scale of the reading in mm. Also, the temperature of the electromagnets could affect the field density as the heat changes the permeability of the electromagnet's material and hence affect the produced electromagnetic field. We concluded that it is possible to increase or decrease the total amount of the electromagnetic field while maintaining the equilibrium as long as the total force is sufficient to overcome the resistive forces.

As the velocity and the precision of motion are important features to determine the targeted areas in the small bowel, we performed various tests to control the motion at different velocities. The velocity can be controlled either by changing the step size that is governed by the total amount of the applied electromagnetic field and the duration of the pulses or by varying the current pulses per unit time (i.e., 1 second). According to (9), and because the total amount of force is

not the same for each step, the current pulse duration is the other parameter that could be varied to choose and maintain the required step size.

It is clear from Fig. 14 that the current pulse duration of each step decreases as the force applied to the capsule increases as described in (9), whereas Fig.15 shows the rate of the pulses per second for 1mm step size to have velocities of 1, 2, 4, 5, 7, and 8mm/s.

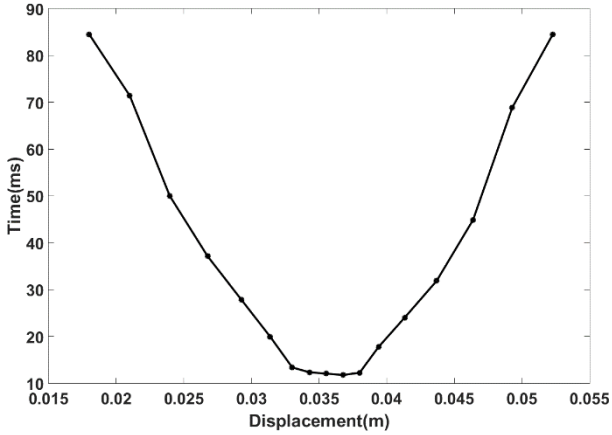

FIGURE 14. The current pulse duration for each step during the traveling in the path shown in Fig.11 (1mm step size at all steps).

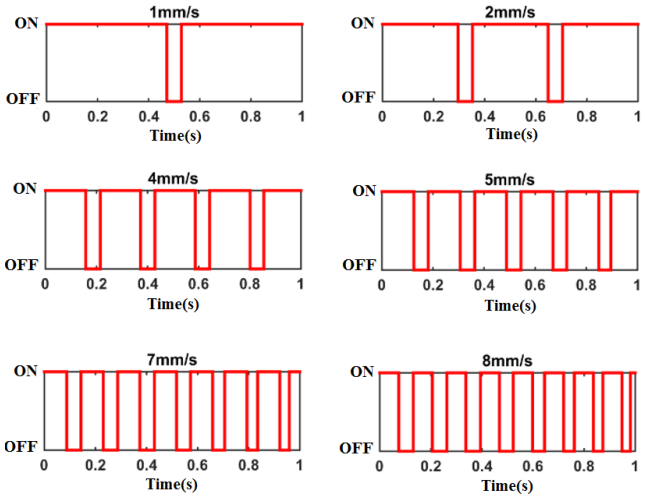

FIGURE 15. The pulses rate applied to the capsule for 1mm step size to change the velocity at 1, 2, 4, 5, 7, and 8 mm/s.

This range of velocity can meet the capsule's motion requirements to be compatible with the GI tract motion and to produce a clear and reasonable number of pictures during motion [14]. We selected the time intervals between the pulses to be equally distributed, and the step size is the same for all steps. Hence, the physician can control the speed; it is not fixed, and it depends on the net force and frequency of the current pulses.

The second approach to assess the control of the velocity is to change the step size. We performed several experiments to move the capsule with different step sizes. Fig. 16 (a) shows a snapshot of the capsule moving in a large step size (25mm), whereas Fig. 16 (b) shows the motion in a small step size (3mm). The controller in the system requires a time between 2 and 4ms (depending on the number of electromagnets used) to calculate and apply the required current according to the new position. The period can be fitted at the rest time between the steps, as Fig.15 shows.

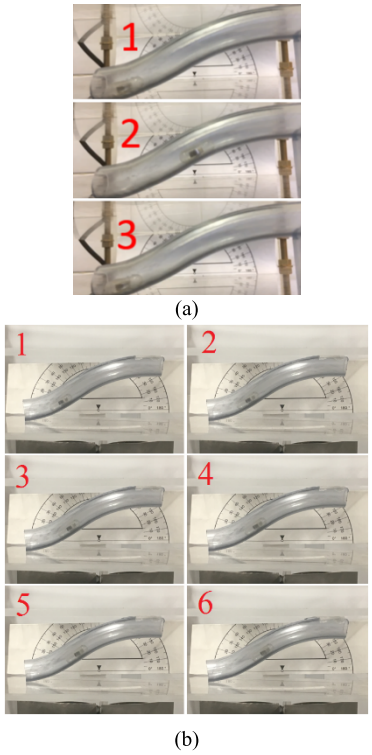

FIGURE 16. The capsule moving in: (a) large step size, (b) smaller step size.

With successful validation of the control system in PVC tubes with different shapes, we implemented an *ex-vivo* demonstration to explore the challenges that could occur in a real environment scenario. The setup used for this experiment is similar to the previous tests, except that we used a fresh pig's intestine in the PVC tube to stimulate the human small intestine environment. We also placed two Layers of minced pig (50mm thickness) above and below the pig's intestine to stimulate human tissue, as Fig.17 shows. For the *ex-vivo*setup, we intended to use the same shape of PVC tube for the previous experiments to differentiate between the setup with the PVC tube only and the *ex-vivo* setup. We then inserted the capsule inside the *ex-vivo* model to test the motion using the approach in Section II.

During this experiment, we noticed that the resistive forces in *ex-vivo* were higher than the forces in the forces in the PVC tube only because of the mucus in the pig's intestine. The friction between the flexible geometry of the pig's intestine and the capsule also increased compared to the rigid geometry of the PVC tube only. As a result, we increased the total force applied to the capsule in *ex-vivo* to maintain the accuracy of each step along the differential tracks, as Fig. 18 shows.

This confirms that a continuous calibration of the position is required in a real environment scenario because the resistive forces and the activities inside the small intestine are not

IEEE Journal of Translational Engineering in Health and Medicine

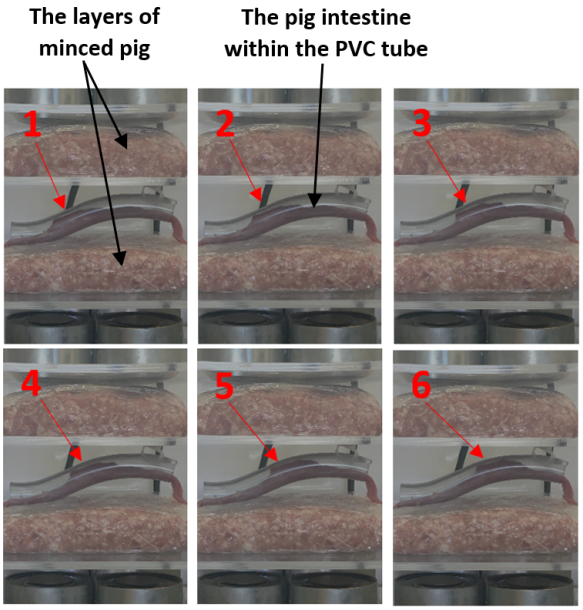

FIGURE 17. The capsule moving in *ex-vivo*at 3*mm* step size with 6 different positions.

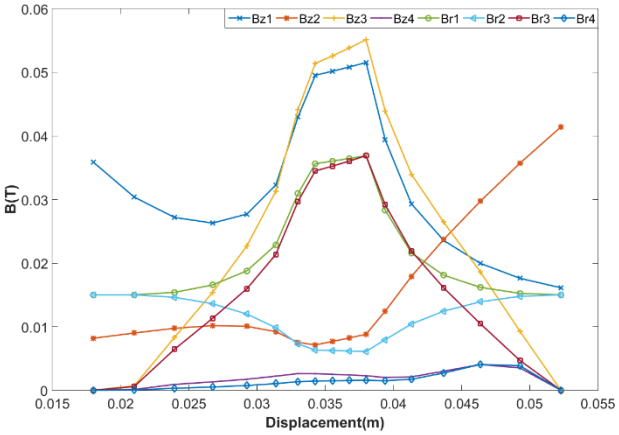

FIGURE 18. *Br* and *Bz* components of the electromagnets at 3*mm* step size in *ex-vivo*.

predictable [14]. This can be done in the proposed system as previously described along with a compatible localization system to confirm the location of each step during the process and calibrate the position if required. In order to investigate the accuracy of the proposed mechanism in this paper, we performed the experiment five times to observe the error in the capsule's motion. Table I shows the errors between the expected location and the actual location after 51 steps with 1mm step size, as visualizing the error for longer distances would be easier than measuring the error for each step.

One unique benefit of digital movement is that it gives a clear and precise comparison of the theoretical and practical results to calibrate the control system if required. The table shows that the range of error is ±2%, which could be acceptable and correctable. Correcting the position can be done by either moving the capsule to the desired location or by adding/subtracting the error in the next step. The variation of the error could occur because of the variation of the resistive

TABLE 1. Errors between the expected location and the actual location.

Experiment No.	1st trial	2nd trial	3rd trial	4th trial	5th trial
Expected distance	51mm	51mm	51mm	51mm	51mm
Actual distance	49.2	51.3	51.1	51.9	52.4
	Mean =51.16			SD=1.26	

TABLE 2. A comparison between def and the other methods.

Method	Recommended Velocity	Power consumption at capsule site	Ability to stop / reverse
Earthworm-like [5]	9.6mm/min	~ 450mW	Yes
Legged-based method [6]	50mm/min	~ 430mW	No
Rotational Magnetic field [7]	1200mm/min	No Power	No
Robotic arm and Hand-held [8]	50mm/min	No Power	Yes
DEF	1 to 480mm/min	No Power	Yes

forces, which proper feedback could overcome. Moreover, the temperature of the electromagnets directly influences the system performance, as the highest error in the fifth trial occurred when the electromagnet's temperatures were around 65°C. Consequently, this system requires a cooling system to run accurately for a long time.

For any wireless capsule locomotion method, it is essential to consider certain factors in order to perform the motion satisfactorily. Controlling the motion at different velocities gives the system the capability to move the capsule conveniently within the GI tract. It also allows the physician to choose the number of pictures or lengths of video per unit length. Moving the capsule at high velocity is undesirable because it increases the resistive forces between the capsule surface and the small bowel, which could cause damage or require more force for motion [26]. The proposed system can change the velocity from 1 to 480mm/min; the capsule's optimum velocity is 150mm/min [16]. Because of the capsule's internal power source limitations, reducing the power consumption required for motion is always preferable. This work makes a trade-off between the capsule and the external magnetic actuation. This is achieved by providing the power externally since an external system will have no major limitations. Since the magnetic field is dynamic, the external power sources does not have a fixed power value. However, it varies from 60 to 280W. Another important factor is system automation and reduction of the human interface. Systems directly controlled by the physician, such as handheld systems, are usually less productive and yield less quality than

automated systems. Automated systems also provide a higher level of safety, whereas the physician's skills and mental state directly influence his or her performance during the process. The ability to hold the capsule at any chosen location and reverse the direction of the motion is important for performing drug delivery or any additional monitoring or diagnosis. Table II compares the proposed method with other methods described in the literature.

IV. CONCLUSION

A new motion mechanism for WCE has been presented and experimentally verified. The system uses a set of dynamically controlled electromagnets that are placed into two platforms below and above the workspace. A combination of analytical and calibration techniques were proposed to achieve high precision of motion. A control strategy is successfully developed to attain an accurate motion at different velocities for forward/backward and inclined paths by maintaining the equilibrium of the forces that are parallel to the direction of motion. The proposed method has been conducted by visualizing the path, however, the capsule need to be navigated by using a feedback system. With long experiments, we observed reasonable differences between the measured and simulated electromagnetic field. The heat has a direct influence on the permeability of the core and hence the produced electromagnetic field. For future enhancement, the systems will utilize a cooling system to maintain the temperature within an acceptable range. Furthermore, a future consideration includes the testing of the mechanism in real environment (i.e., *in vivo*) to explore any further requirements and challenges.

ACKNOWLEDGMENT

The authors would like to express our appreciation to Mr.Taiyang Wu for the helping during this work.

REFERENCES

[1] G. Iddan, G. Meron, A. Glukhovsky, and P. Swain, "Wireless capsule endoscopy," *Nature*, vol. 405, p. 417, May 2000.

[2] B. H. K. Leung *et al.*, "A therapeutic wireless capsule for treatment of gastrointestinal haemorrhage by balloon tamponade effect," *IEEE Trans. Biomed. Eng.*, vol. 64, no. 5, pp. 1106–1114, May 2017.

[3] L. Lu, G. Yan, X. Kong, K. Zhao, and F. Xu, "Colonic motility analysis using the wireless capsule," *IEEE Sensors J.*, vol. 16, no. 9, pp. 3272–3281, May 2016.

[4] M. R. Yuce, G. Alici, and T. D. Than, "Wireless endoscopy," *Wiley Encyclopedia of Electrical and Electronics Engineering*. Hoboken, NJ, USA: Wiley, 2015.

[5] D. Hosokawa, T. Ishikawa, H. Morikawa, Y. Imai, and T. Yamaguchi, "Development of a biologically inspired locomotion system for a capsule endoscope," *Int. J. Med. Robot. Comput. Assist. Surg.*, vol. 5, no. 4, pp. 471–478, Dec. 2009.

[6] P. Valdastri, R. J. Webster, C. Quaglia, M. Quirini, A. Menciassi, and P. Dario, "A new mechanism for mesoscale legged locomotion in compliant tubular environments," *IEEE Trans. Robot.*, vol. 25, no. 5, pp. 1047–1057, Oct. 2009.

[7] M. Sendoh, K. Ishiyama, and K. I. Arai, "Fabrication of magnetic actuator for use in a capsule endoscope," *IEEE Trans. Magn.*, vol. 39, no. 5, pp. 3232–3234, Sep. 2003.

[8] G. Ciuti, P. Valdastri, A. Menciassi, and P. Dario, "Robotic magnetic steering and locomotion of capsule endoscope for diagnostic and surgical endoluminal procedures," *Robotica*, vol. 28, no. 2, pp. 199–207, Oct. 2009.

[9] G.-S. Lien, C.-W. Liu, J.-A. Jiang, C.-L. Chuang, and M.-T. Teng, "Magnetic control system targeted for capsule endoscopic operations in the stomach—Design, fabrication, and *in vitro* and *ex vivo* evaluations," *IEEE Trans. Biomed. Eng.*, vol. 59, no. 7, pp. 2068–2079, Jul. 2012.

[10] F. N. Alsunaydih, J.-M. Redoute, and M. R. Yuce, "Improving resolution of robotic capsule locomotion using dynamic electromagnetic field," in *Proc. 38th Annu. Int. Conf. IEEE Eng. Med. Biol. Soc. (EMBC)*, Orlando, FL, USA, Aug. 2016, pp. 219–222.

[11] H. Keller *et al.*, "Method for navigation and control of a magnetically guided capsule endoscope in the human stomach," in *Proc. 4th IEEE RAS EMBS Int. Conf. Biomed. Robot. Biomechatron. (BioRob)*, Rome, Italy, Jun. 2012, pp. 859–865.

[12] C. Lee *et al.*, "Active locomotive intestinal capsule endoscope (ALICE) system: A prospective feasibility study," *IEEE/ASME Trans. Mechatronics*, vol. 20, no. 5, pp. 2067–2074, Oct. 2015.

[13] T. D. Than, G. Alici, H. Zhou, and W. Li, "A review of localization sagesystems for robotic endoscopic capsules," *IEEE Trans. Biomed. Eng.*, vol. 59, no. 9, pp. 2387–2399, Sep. 2012.

[14] L. Lu, G. Yan, K. Zhao, and F. Xu, "Analysis of the chaotic characteristics of human colonic activities and comparison of healthy participants to costive subjects," *IEEE J. Biomed. Health Informat.*, vol. 20, no. 1, pp. 231–239, Jan. 2016.

[15] H. Mateen, R. Basar, A. U. Ahmed, and M. Y. Ahmad, "Localization of wireless capsule endoscope: A systematic review," *IEEE Sensors J.*, vol. 17, no. 5, pp. 1197–1206, Mar. 2017.

[16] L. Liu, S. Towfighian, and A. Hila, "A review of locomotion systems for capsule endoscopy," *IEEE Rev. Biomed. Eng.*, vol. 8, pp. 138–151, 2015.

[17] E. P. Furlani, "A method for predicting the field in axial field motors," *IEEE Trans. Magn.*, vol. 28, no. 5, pp. 2061–2066, Sep. 1992.

[18] A. Moglia, A. Menciassi, and P. Dario, "Recent patents on wireless capsule endoscopy," *Recent Patents Biomed. Eng.*, vol. 1, no. 1, pp. 24–33, 2008.

[19] V. Labinac, N. Erceg, and D. Kotnik-Karuza, "Magnetic field of a cylindrical coil," *Amer. J. Phys.*, vol. 74, no. 7, pp. 621–627, 2006.

[20] F. Carpi, S. Galbiati, and A. Carpi, "Controlled navigation of endoscopic capsules: Concept and preliminary experimental investigations," *IEEE Trans. Biomed. Eng.*, vol. 54, no. 11, pp. 2028–2036, Nov. 2007.

[21] G. Ciuti, A. Menciassi, and P. Dario, "Capsule endoscopy: From current achievements to open challenges," *IEEE Rev. Biomed. Eng.*, vol. 4, pp. 59–72, Oct. 2011.

[22] J. D. Jackson, *Classical Electrodynamics*. New York, NY, USA: Wiley, 1966, p. 283.

[23] P. Dario and C. A. Mosse, "Review of locomotion techniques for robotic colonoscopy," in *Proc. IEEE Int. Conf. Robot. Autom.*, Sep. 2003, pp. 1086–1091.

[24] F. N. Alsunaydih, J. M. Redoute, and M. R. Yuce, "A wireless capsule endoscopy steering mechanism using electromagnetic field platform," in *Proc. 39th Annu. Int. Conf. IEEE Eng. Med. Biol. Soc. (EMBC)*, Seogwipo, South Korea, 2017, pp. 3036–3039.

[25] X. Wang and M. Meng, "An experimental study of resistant properties of the small intestine for an active capsule endoscope," *Proc. Inst. Mech. Eng., H, J. Eng. Med.*, vol. 224, no. 1, pp. 107–118, 2009.

[26] N.-K. Baek, I.-H. Sung, and D.-E. Kim, "Frictional resistance characteristics of a capsule inside the intestine for microendoscope design," *Proc. Inst. Mech. Eng., H, J. Eng. Med.*, vol. 218, no. 3, pp. 193–201, Jan. 2004.

[27] F. Xu and G. Yan, "Toward a wireless electronic capsule with microsensors for detecting dysfunction of human gastric motility," *IEEE Sensors J.*, vol. 15, no. 4, pp. 2194–2202, Apr. 2015.

[28] J. S. Kim, I. H. Sung, Y. T. Kim, D. E. Kim, and Y. H. Jang, "Analytical model development for the prediction of the frictional resistance of a capsule endoscope inside an intestine," *Proc. Inst. Mech. Eng., H, J. Eng. Med.*, vol. 221, no. 8, pp. 837–845, Jan. 2007.

[29] A. Moglia, A. Menciassi, M. O. Schurr, and P. Dario, "Wireless capsule endoscopy: From diagnostic devices to multipurpose robotic systems," *Biomed. Microdevices*, vol. 9, no. 2, pp. 235–243, Apr. 2007.

[30] Y. Fu, W. Zhang, M. Mandal, and M. Q.-H. Meng, "Computer-aided bleeding detection in WCE video," *IEEE J. Biomed. Health Informat.*, vol. 18, no. 2, pp. 636–642, Mar. 2014.

[31] J. J. Abbott, O. Ergeneman, M. P. Kummer, A. M. Hirt, and B. J. Nelson, "Modeling magnetic torque and force for controlled manipulation of soft-magnetic bodies," *IEEE Trans. Robot.*, vol. 23, no. 6, pp. 1247–1252, Dec. 2007.